Eur. Phys. J. C (2025) 85:254
https://doi.org/10.1140/epjc/s10052-025-13986-5

THE EUROPEAN PHYSICAL JOURNAL C

Regular Article - Theoretical Physics

Searching for cosmic-time variation in the gravitational constant with strongest H_2 Werner transitions

T. D. Le[1,2,a]

[1] Division of Applied Physics, Dong Nai Technology University, Bien Hoa City, Vietnam
[2] Faculty of Engineering, Dong Nai Technology University, Bien Hoa City, Vietnam

Received: 28 July 2024 / Accepted: 22 February 2025

Abstract Probing changes in fundamental physics constants over cosmological space-time is a significant area in both theoretical and experimental physics. An effective method for probing these variations is to compare laboratory measurements with astrophysical data. In this study, we utilize a combination of laboratory data and observed Werner transitions of H_2 in the white dwarf star GD29-38. Our analysis reveals that the temporal variation of the gravitational constant is $\dot{G}/G = (0.014 \pm 0.096) \times 10^{-15}$ year^{-1}, with a gravitational potential of $\phi \approx 1.9 \times 10^4$ and an average total redshift of H_2 of $z_{\rm abs} = 0.0001360(8)$. This newly established constraint on the time variation of G plays a crucial role in enhancing discussions within unified theories.

1 Introduction

One of the foundational aspects of General Relativity, known as the equivalence principle, claims that fundamental constants remain unchanged regardless of their spatial location. However, contemporary grand-unification theories provide a significant context to this principle by suggesting that these constants might operate as dynamic scalar fields with low mass [1]. If these theories are accurate, it implies that these constants could experience slow variations over cosmological distances and timescales, adding a location-dependent dimension to their values [2]. In recent years, substantial efforts have been dedicated to constraining the variability of the fine structure constant, as documented in comprehensive reviews [3,4], which have established stringent upper limits on its rate of change. In contrast, the potential variation of the gravitational constant G has received relatively limited attention, likely due to the difficulties associated with its precise measurement [5]. Notably, G is the fundamental constant with the least precise determination, evidenced by significant disparities across multiple measurements.

Exploring the variations of fundamental constants over space-time is essential for advancing modern physics and understanding phenomena beyond the Standard Model (SM). Astrophysical and cosmological observations are powerful tools for investigating these intriguing phenomena. Recent studies have proposed unified scenarios involving variations in fundamental physical constants such as α, μ, and G [6–8]. Thus, investigating the spatial and temporal effects on the gravitational constant G is crucial for the development of unification theories. The most stringent constraints on the variation rate of G, denoted as $\dot{G}/G = (2 \pm 7) \times 10^{-13}$ year^{-1}, come from Lunar Laser Ranging, though these constraints are inherently local [9]. Additional constraints are provided by the Hubble diagram of Type Ia supernovae at intermediate cosmological ages, which places $\dot{G}/G \sim 10^{-11}$ year^{-1} at $z \sim 0.5$ [10]. Finally, Big Bang Nucleosynthesis offers limits on possible variations in the gravitational constant, ranging from -3×10^{-11} year^{-1} to 4×10^{-13} year^{-1} [11]. White dwarfs provide a natural method for constraining potential variations in the gravitational constant, G. This capability is due to several factors. Firstly, white dwarfs have exceptional longevity, making them sensitive to even small rates of change in G. Secondly, as the final evolutionary stage for most stars, white dwarfs are plentiful in the universe. Thirdly, their compact nature results in a structure that is highly responsive to the precise value of G. Lastly, the well-understood evolution of white dwarfs can be precisely characterized as a straightforward gravothermal process, where their luminosity is primarily determined by the delicate balance between thermal and gravitational energies. As a result, any secular variation in G significantly impacts the gravothermal equilibrium of white dwarfs, thereby affecting their luminosities. An interesting method to utilize white dwarfs for

[a] e-mail: leducthong@dntu.edu.vn (corresponding author)

Published online: 10 March 2025

constraining variations in G involves estimating how the secular rate of change in the pulsation period of variable white dwarfs depends on their cooling rate [12]. Research suggests that this rate of change depends not only on the cooling rate but also on the rate of variation in the gravitational constant G. Applying this approach to the well-studied variable white dwarf G117-B15A provided a broad constraint: $-2.5 \times 10^{-10}\,\text{year}^{-1} \leq \dot{G}/G \leq 0$ [13]. Another study to constrain G-variation involves examining the white dwarf luminosity function. The abundance of white dwarfs is closely linked to the characteristic cooling time within the corresponding luminosity range, thereby influencing the cut-off position of the white dwarf luminosity function at low luminosities. Researchers employed a simplified model to investigate the potential effects of a slowly varying G on the white dwarf luminosity function [14]. Assuming that G is low enough for white dwarfs to rapidly adjust their mechanical structure compared to the cooling timescale, the implications were determined using principles of mixing energy [14,15].

In this study, we investigate how cosmological variations in space-time might affect the gravitational constant, focusing on spectral observations of Werner transitions of H_2 in the white-dwarf star GD29-38 [16–18]. The spectrum of GD29-38, captured by the *Cosmic Origins Spectrograph* aboard the *Hubble Space Telescope*, reveals a gravitational potential approximately 10^4 times stronger than what is observed in Earth-based experiments. This strong gravitational field makes GD29-38 an excellent candidate for setting an upper limit on the variation of the gravitational constant over cosmological timescales. Our study estimates potential cosmological deviations with a precision of $\dot{G}/G = (0.014 \pm 0.096) \times 10^{-15}\,\text{year}^{-1}$, comparable to the precision achieved in previous studies [19–22].

2 $\dot{G}/G$ constrained by the strongest H_2 Werner transitions

The spectra of white-dwarf stars provide a framework for exploring phenomena beyond the Standard Model of cosmology and particle physics. This framework helps identify contemporary variations in several fundamental constants, including the fine-structure constant (α), the proton-to-electron mass ratio (μ), and the gravitational constant (G). Previous studies have detailed the gravitational surface potential, ϕ, at a distance r from an object's mass M, expressed as $\phi = \frac{GM}{rc^2}$. These models involve scalar fields and related interactions influenced by the gravitational redshift effect within the general relativity framework. Thus, the energy loss (E) of a photon escaping a gravitational surface (r) can be represented as $z = -\frac{\Delta E}{E} = -\frac{\phi}{c^2}$, where the fractional change in energy correlates with the fractional change in observational wavelengths, $-\frac{\Delta E}{E} = \frac{\Delta\lambda}{\lambda} \sim \frac{\Delta\alpha}{\alpha}$. This method has been used to study cosmological variations in fundamental constants such as the fine-structure constant (α) under high surface gravity conditions [19–26]. Gravitational redshift traditionally refers to the shift in light caused by a gravitational field. However, recent studies have uncovered a deeper connection between gravitational redshift and variations in the fine-structure constant (α), particularly in high-energy environments. For instance, Hu et al. [27] demonstrated that changes in α can affect atomic energy levels, leading to shifts in spectral lines that manifest as redshifts. In regions with strong gravitational fields, such as near black holes or other massive objects, scalar fields driving variations in α can result in observable changes in redshift. These effects have been modeled theoretically in various works [24,26,28]. Thus, while the link between gravitational redshift and fine-structure constant variation is indirect, it is well-supported by both observational and theoretical frameworks, particularly when analyzing high-redshift quasar data where gravitational effects and variations in α coexist.

An effective way to probe these variations involves a dimensionless constant, often denoted as α, grounded in Grand Unified Theories (GUTs). Temporal or spatial variations in fundamental constants might unify gravitational and electromagnetic forces. Assuming uniform variations in related Yukawa couplings and using dimensional transmutations to establish a weak scale, these couplings are expressed through a driven dilaton-type mechanism. Thus, the relationship between variations in the fine-structure constant and the Quantum Chromodynamics (QCD) scale (Λ_{QCD}) is denoted as [29,30].

$$\frac{\Delta\Lambda_{\text{QCD}}}{\Lambda_{\text{QCD}}} = R\frac{\Delta\alpha}{\alpha} \tag{1}$$

where R is determined by the Grand Unified Theory (GUT). The value of R is derived from the relationship

$$\alpha(M_{\text{GUT}}) = \alpha_s(M_{\text{GUT}}) \tag{2}$$

and is model-independent at low energies. Simultaneously, changes in Yukawa couplings (h) lead to modifications in the Higgs Vacuum Expectation Value (v) at the Planck mass scale of GUTs. Consequently,

$$v = M_{\text{Planck}} \exp\left(-\frac{8\pi^2 c}{h^2}\right) \tag{3}$$

and

$$\frac{\Delta v}{v} = 16\pi^2 c\frac{\Delta h}{h} = S\frac{\Delta h}{h} \rightarrow \frac{\Delta v}{v} = S\frac{\Delta h}{h} \tag{4}$$

where $S = \frac{d\ln\nu}{d\ln h}$, and $\frac{\Delta h}{h} = \frac{1}{2}\frac{\Delta\alpha}{\alpha}$ (with $c \approx \hbar \approx 1$). Thus,

$$\frac{\Delta m_e}{m_e} = \frac{1}{2}(1+S)\frac{\Delta\alpha}{\alpha} \tag{5}$$

and

$$\frac{\Delta m_p}{m_p} = [1.6R + 0.4(1+S)]\frac{\Delta\alpha}{\alpha} \tag{6}$$

correspond to variations in the electron mass and the proton-to-electron mass ratio, respectively. Using a perturbative approach, the variations in neutron mass (m_n) and average nucleon mass (m_N) are given by

$$\frac{\Delta m_n}{m_n} = \frac{\Delta m_N}{m_N} = \frac{\Delta m_p}{m_p} \tag{7}$$

These assumptions lead to the following relationship between α and G [19–22,29,30]:

$$\frac{\Delta G}{G} = [1.6R + 0.4(1+S)]\frac{\Delta\alpha}{\alpha} \tag{8}$$

The parameters R and S are treated as free parameters, and their absolute values depend on the model used. These parameters are constrained by observational data, and variations are linked to the parameters α, μ, and G. The outcomes are sensitive to prior choices, with a broader parameter space generally leading to smaller preferred values for R and S. A more general initial choice increases the fraction of the parameter space with larger values of R or S. Consequently, our study emphasizes constraining a uniform prior for R and S. Observational data are used to determine R or S, treating them as free phenomenological parameters within unification scenarios. Alternatively, both parameters can be derived directly from astrophysical data or laboratory measurements. We have analyzed models with specific values of R and S, but in general, these values can vary unless marginalized. In our analysis, we explored models with varying R and S values to assess their impact on the gravitational constant G. In the absence of specific constraints, these parameters were allowed to vary within certain limits. To refine our focus and provide a solid basis for our investigation, we carefully considered the range of possible values. To determine the most likely values for R and S, we used constraints derived from equations specific to our study. These constraints represented the complex interplay between the parameters and the underlying physical phenomena. The relations were expressed mathematically as follows:

$$0.80R - 0.30(1+S) = -0.81 \pm 0.85 \tag{9}$$

$$0.10R - 0.04(1+S) = -1.96 \pm 1.79 \tag{10}$$

These equations introduce degeneracy directions in our study. Our statistical evaluation involved an in-depth exploration of error determination, considering the potential presence of multiple minima. The nonlinear-least-squares (NLS) algorithm played a critical role in minimizing discrepancies between our theoretical predictions and the observed data. We meticulously selected a function within the family of NLS algorithms to align with our study objectives. Additionally, we conducted a comprehensive analysis of the data's distributional characteristics, recognizing the inherent positivity in both spectra and wavelengths. We evaluated the assumption of a Gaussian distribution for error estimation and explicitly addressed any observed non-Gaussian patterns. This thorough examination aimed to provide a solid foundation for the statistical significance of our results. Our rigorous analysis included advanced optimization techniques, constraints derived from specific relations, error estimation, and careful consideration of data distribution characteristics. These efforts collectively contributed to the robustness and statistical significance of our parameter estimation process. After this detailed analysis, we found that the parameters $R = 273 \pm 86$ and $S = 603 \pm 230$ best align with our research objectives. These values were not selected arbitrarily but were determined through a systematic optimization process, considering both the theoretical framework and compatibility with observational data. Therefore, the parameters $R = 273 \pm 86$ and $S = 603 \pm 230$ are chosen as the best fit for our study, consistent with ranges explored in references [19–22,29,30]. While these estimations aim to provide best-fit values, the exact selection of R and S may vary depending on the specific unified scenarios considered. By choosing these particular values, we establish a well-defined set of conditions that facilitate a thorough investigation of the secular variation of the gravitational constant (G) within a manageable parameter space. This approach enhances the robustness of our study and ensures that our results are grounded in a careful consideration of theoretical expectations and empirical constraints. Comparing the Werner transition lines of H_2 observed in the white dwarf GD29-38 spectrum with laboratory measurements allows us to assess the effect of the gravitational constant (G)'s time variation over cosmological timescales. The spectrum of GD29-38, recorded by the *Cosmic Origins Spectrograph* aboard the *Hubble Space Telescope*, exhibits a gravitational potential $\phi \approx 1.9 \times 10^4$ and an average total redshift of H_2 of $z_{\rm abs} = 0.0001360(8)$. Fitting procedures indicate that the parameters R and S are consistent with values found in other studies [16,19–22,29–31].

The variation of the gravitational constant G was estimated using measurement data for α, R, and S, with uncertainties propagated through standard error propagation techniques [32,33]. The error in G was calculated using the rela-

tion

$$\delta(\Delta G) = \sqrt{\left(\frac{\partial f}{\partial \alpha}\delta\alpha\right)^2 + \left(\frac{\partial f}{\partial R}\delta R\right)^2 + \left(\frac{\partial f}{\partial S}\delta S\right)^2}, \quad (11)$$

ensuring that the final uncertainty in G properly accounts for the uncertainties in each measured variable. Our analysis employed a non-linear least squares (NLS) algorithm, a sophisticated optimization technique effective for finding best-fit parameters in mathematical models. This method, well-established in fields such as astrophysics [34,35], was used to refine model parameters through an iterative process, minimizing discrepancies between theoretical predictions and observational data from the white dwarf spectrum. The spectral lines of molecular hydrogen (H_2) in the white dwarf GD29-38, known for their narrow and symmetric profiles, were particularly valuable for this analysis. Gaussian line-fitting profiles were used to determine linewidths and central velocities, with single Gaussian fits for individual velocity components and multiple Gaussians for multi-component lines. Key parameters, including the column density (N), absorption redshift ($z_{\rm abs}$), and Doppler linewidth ($b = \sqrt{2}\sigma$), were derived from these profiles.

Simulations of the H_2 lines were conducted to identify $\Delta\alpha/\alpha$-values, which, along with R and S, provided input for determining the variation of G. The fitting procedure for $\dot{G}/G$ utilized χ^2 minimization, with the minimum $\chi^2_{\rm min}$ found through a reduced approximation of $\Delta\chi^2 = 1$. A one-sigma error on $\dot{G}/G$ was assigned using the criterion $\Delta\chi^2 = \chi^2 - \chi^2_{\rm min} = 1$, which also enabled the evaluation of the maximum change rates of G. This method provided crucial insights into potential cosmological variations in the gravitational constant (G) over time. The Gaussian distribution framework was further employed to estimate both statistical and systematic errors, capturing the interplay between various uncertainty sources. By leveraging this statistical approach, the study achieved a detailed characterization of uncertainties, enhancing the robustness and validity of the conclusions regarding the secular variation of G in strong gravitational fields, such as those in white dwarf stars.

Table 1 presents the statistical and systematic errors calculated ($\sigma^2_{\rm total} = \sigma^2_{\dot{G}/G} + \sigma^2_{\rm sys}$) for the $\dot{G}/G$ values. Figure 1 illustrates the distribution of z versus gravitational redshift, which tests the bounds on dimensionless fundamental physical constants (α, G). Various inconsistencies were observed across different methods for determining systematic errors. It is acknowledged that some evidence is not fully controlled or sufficiently understood. Variations in results across observational studies can arise from different analysis methods and uncertainties in laboratory wavelength measurements [19,20,22,29,30,34–38]. Our analysis combined observed spectra with an uncertainty of $\sim 1 \times 10^{-6}$ and laboratory wavelengths with an uncertainty of $\sim 1 \times 10^{-7}$ using NLS algorithm. This method is highly effective for parameter optimization. We used the Gaussian distribution to estimate α-errors with high precision, improving accuracy in measuring possible α-changes compared to previous works. The assumption of a Gaussian distribution for error estimation was crucial, but it is important to address the nature of our data. Both spectra and wavelengths involve positive values, whereas the Gaussian distribution spans both positive and negative ranges. To evaluate the appropriateness of the Gaussian assumption, we thoroughly examined the distributional characteristics of our data. We considered the positivity of the data and any potential deviations from a strictly Gaussian form. We will provide a detailed description of observed patterns or non-Gaussian features in our data and any adjustments made to account for these deviations in our modeling and analysis.

Our study builds on previous research by proposing that highly-resolved white-dwarf spectra offer one of the tightest constraints on the potential spatial and temporal variation of G, particularly within the context of Grand Unified Theories (GUTs) that link $\Delta\alpha/\alpha$ to $\dot{G}/G$.

Table 1 Measurements of $\dot{G}/G$ at various redshifts with an average total redshift of H_2, $z_{\rm abs} = 0.0001360(8)$

Line	$\lambda_{\rm Obser}$ (Å)	$\dot{G}/G$ [10^{-15} year^{-1}]	$\sigma_{\dot{G}/G}$ [10^{-15} year^{-1}]
Q(19)	1142.712 (1)	0.06130	0.07000
Q(13)	1143.692 (1)	− 0.03327	− 0.09024
P(13)	1151.641 (1)	0.02426	0.07500
P(19)	1152.290 (1)	0.03835	0.08000
Q(15)	1156.072 (1)	0.02500	0.07000
Q(21)	1158.244 (1)	− 0.05485	0.09850
P(15)	1164.871 (1)	0.03539	0.06120
P(21)	1168.414 (1)	− 0.09545	0.10120
Q(17)	1169.257 (1)	− 0.06000	0.10250
P(23)	1184.811 (1)	− 0.05800	0.08500

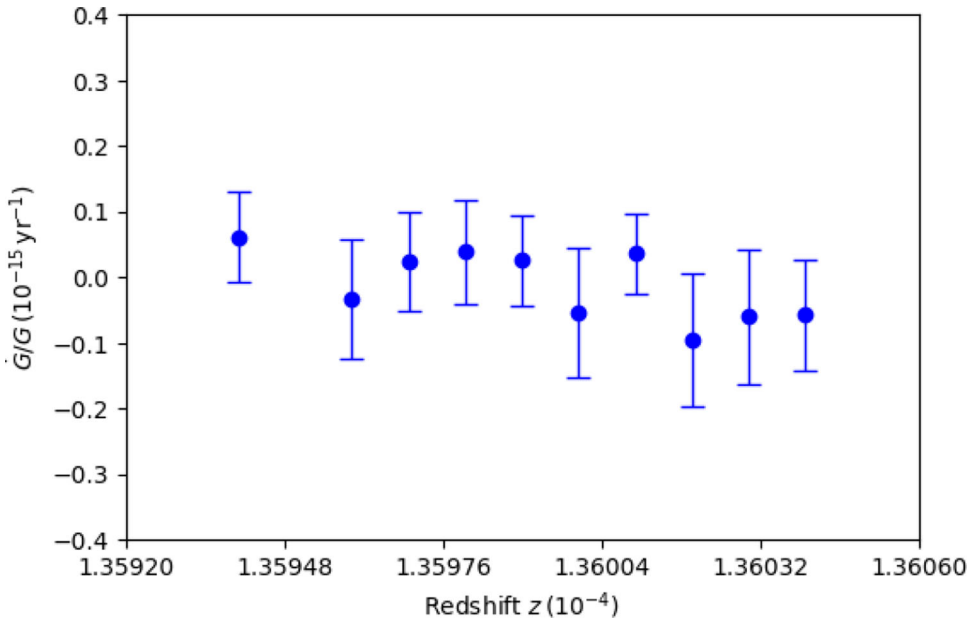

Fig. 1 Distribution of $\dot{G}/G$ versus gravitational redshift. Each point represents one of the 10 strongest lines from the spectral lines of the white dwarf GD29-38, used in analyzing the Werner transitions of hydrogen. Our final result, $\dot{G}/G = (0.014 \pm 0.096) \times 10^{-15}\,\mathrm{year}^{-1}$, was determined through the analysis of the data presented in this figure. This figure summarizes essential information integral to our study and reveals trends that led to our conclusion

The primary objective of our study was to demonstrate that white dwarfs can constrain variations in fundamental constants, including the fine-structure constant, the proton-to-electron mass ratio, and the gravitational constant. Our analysis supports the idea of potential cosmological variations in the gravitational constant over time. Specifically, based on our examination of the Werner transitions of H_2, our results establish a fractional change in the gravitational constant of $\dot{G}/G = (0.014 \pm 0.096) \times 10^{-15}\,\mathrm{year}^{-1}$ over the gravitational redshift $z_{\mathrm{abs}} = 0.0001360(8)$. Our findings, considering current constraints from observational data and laboratory measurements, suggest a promising approach toward understanding variations in fundamental physical constants [19,20,22,29,30,34–38].

3 Discussions

Theoretical frameworks in fundamental physics propose that fundamental constants may change across cosmic time and space. Specifically, light scalar fields responsible for these fluctuations could lead to variations in fundamental constants influenced by local gravitational fields. Recent studies have explored these phenomena to investigate potential links between fundamental constants such as the fine-structure constant (α), the proton-to-electron mass ratio (μ), and the gravitational constant (G), particularly within the intense gravitational fields present in the photosphere of white dwarf stars [10,13,39]. Pulsating white dwarfs, such as G117-B15A, and white dwarf asteroseismology have contributed to the exploration of G-variations, yielding constraints of $|\dot{G}/G| \leq 4.10 \times 10^{-10}\,\mathrm{year}^{-1}$ [28,40–45]. Gravitational waves and pulsar binaries, such as PSR1913+16, have also been used to set constraints on $\dot{G}/G$ ranging from $1.3 \times 10^{-10}\,\mathrm{year}^{-1}$ to $\sim -1.8 \times 10^{-10}\,\mathrm{year}^{-1}$ [46–49]. Additionally, data from six telescopes, particularly through mode spectra, have provided further constraints on the time-dependent variation of $\dot{G}/G$ ranging from $\leq 10^{-10}\,\mathrm{year}^{-1}$ to $\sim -1.8 \times 10^{-12}\,\mathrm{year}^{-1}$. White dwarf cooling theory has also been employed, showing time variations in G within the range of $\dot{G}/G \leq 10^{-10}\,\mathrm{year}^{-1}$ and $\dot{G}/G \sim -1.8 \times 10^{-12}\,\mathrm{year}^{-1}$ [50–57]. However, other investigations, particularly those utilizing pulsating white dwarfs like G117-B15A and R548, have reported less stringent limits on the time variation of $\dot{G}/G \sim -1.3 \times 10^{-10}\,\mathrm{year}^{-1}$ [58–60]. Gravitational waves have set new limits on the time variation of $\dot{G}/G$, with findings around $\sim 10^{-11}\,\mathrm{year}^{-1}$ [61]. Similarly, for the pulsar binary PSR1913+16, the Brans-Dicke theory analysis yielded a limit of $\dot{G}/G = (1.0 \pm 2.3) \times 10^{-11}\,\mathrm{year}^{-1}$. Subsequent studies refined these limits to $\dot{G}/G = (4 \pm 5) \times 10^{-12}\,\mathrm{year}^{-1}$ and $\dot{G}/G = (-0.9 \pm 1.8) \times 10^{-11}\,\mathrm{year}^{-1}$, incorporating data from various sources including the quasar PSR B1855+09 [1,62].

Furthermore, the potential effects of space or time-varying G have been investigated through comparisons of data from six telescopes. Mode spectra analysis has led to more substantial constraints of $|\dot{G}/G| < 1.6 \times 10^{-12}\,\mathrm{year}^{-1}$ at a two-sigma level. Consistently, studies report that the time-dependent effect $\dot{G}/G = (-6 \pm 42) \times 10^{-13}\,\mathrm{year}^{-1}$ does not exceed the $10^{-12}\,\mathrm{year}^{-1}$ level, underscoring the robustness of this conclusion [63]. Measuring the wavelength shift of absorption lines in the photosphere of white dwarfs, based on the ratio of stellar mass to radius, provides a method to estimate gravitational redshift. However, isolating this gravitational redshift is challenging due to the presence of Doppler shifts caused by random stellar motions along the line of

sight. To address this, the use of co-moving companions can help distinguish between Doppler and gravitational redshifts, thereby allowing for the constraint of velocity components such as radial velocity in white dwarfs. By measuring the mean gravitational redshift across a sample of field white dwarfs and accounting for Doppler effects due to random stellar motions, it is possible to derive relationships between white dwarf mass and radius, as well as their surface temperatures. The spectra of white dwarfs, characterized by photospheric lines, pressure conditions, and effective temperatures, provide crucial information for this analysis. In the case of the white dwarf star GD29-38, previous best-fit analyses of its spectrum provide a basis for estimating physical conditions. The spectrum of H_2 is applied and related to each object before fitting for gravitational redshift estimation. This procedure considers uncertainties around $1:10^6$ for the spectra and $1:10^7$ for laboratory wavelength measurements.

In the fitting procedure, parameters such as (N, $z_{\rm abs}$, $b = \sqrt{2}\sigma$) are used, assuming that components correspond to the same transitions for all Lyman transitions of H_2. The redshift scale or velocity is employed to determine the positions of H_2 lines. Typically, $\dot{G}/G$ is used as a fit parameter, with $\dot{G}/G$ values derived from the shifted transitions of H_2 lines for each spectral line. The H_2 lines are particularly suitable for analysis due to their frequent presence in white dwarf spectra and their high sensitivity for testing physical constants like the gravitational constant. The small line separations of H_2 lines in the current analysis help minimize systematic effects, allowing for the accurate detection of spatial or temporal variations in G.variations in G with high accuracy.

4 Conclusions

In this study, we investigate the secular variation of the gravitational constant (G) using the formula:

$$\frac{\Delta G}{G} = [1.6R + 0.4(1+S)]\,\frac{\Delta\alpha}{\alpha} \tag{12}$$

where $\frac{\Delta G}{G}$ denotes the relative change in the gravitational constant, R and S are parameters obtained from our fitting program, and $\frac{\Delta\alpha}{\alpha}$ represents the relative change in the fine-structure constant.

Our analysis, grounded in white dwarf spectra, provides a more precise upper limit for the secular variation of G compared to previous methods such as pulsar timing, lunar laser ranging, Big Bang nucleosynthesis, and the ages of globular clusters. Notably, our results integrate empirical data with assumptions about spatial or temporal extra-dimensions [1,60–66].

In comparison to the study by Garcia-Berro et al. [67], our research offers several advancements:

- **Improved data quality:** We utilize more recent and higher-quality spectral data from the white dwarf GD29-38. This enhancement provides greater precision in measuring the Werner transitions, crucial for determining the secular variation of G.
- **Advanced modeling techniques:** Our study employs updated atomic data and sophisticated modeling techniques, resulting in a more accurate spectral analysis.
- **Targeted approach:** Unlike Garcia-Berro et al. [67], which provided a broad analysis using various astrophysical methods, our research focuses specifically on white dwarf spectra, allowing for a more refined approach.

Our findings present a more precise upper limit for $\dot{G}/G$, specifically $\dot{G}/G = (0.014 \pm 0.096) \times 10^{-15}\,\text{year}^{-1}$, with a gravitational potential of $\phi \approx 1.9 \times 10^4$ and an average total redshift of H_2 of $z_{\rm abs} = 0.0001360(8)$, offering a narrower uncertainty range compared to previous studies. These improvements highlight the novelty and significance of our work in providing tighter constraints on the temporal variations of the gravitational constant.

From a broader theoretical perspective, exploring spatial or temporal variations in fundamental dimensionless couplings (α, μ, and G) could advance beyond conventional astrophysical and cosmological models. The inclusion of our derived formula enhances the clarity of our approach and links our findings directly to theoretical frameworks. Our investigation also suggests that deviations in G might provide insights into the incompleteness of the Equivalence Principle (EEP).

Future studies will focus on refining our understanding of these constants using additional astrophysical sources, such as Cosmic Microwave Background data, Big Bang Nucleosynthesis data, and exploring the brane-world-type unification scenarios. As the quality of astrophysical observations and data improves, we anticipate that our findings will contribute further insights into the realms of Grand Unified Theories (GUTs) [63,68–70].

Funding This research received no external funding.

Data Availability Statement All data generated or analyzed during this study are included in these published articles [17,18].

Code Availability Statement This manuscript has no associated code/software. [Author's comment: Code/Software sharing not applicable to this article as no code/software was generated or analysed during the current study].

Declarations

Conflict of interest The authors declare that we have no conflict of interest.

Funded by SCOAP[3].

References

1. P. Loren-Aguilar, E. Garcia-Berro, J. Isern, Y.A. Kubyshin, Time variation of G and alpha within models with extra dimensions. Class. Quantum Gravity **20**, 3885–3896 (2003). https://doi.org/10.1088/0264-9381/20/18/302. arXiv:astro-ph/0309722
2. E. Teller, On the change of physical constants. Phys. Rev. **73**, 801–802 (1948). https://doi.org/10.1103/PhysRev.73.801
3. J.-P. Uzan, Varying constants, gravitation and cosmology. Living Rev. Relativ. **14**(2), 1–155 (2011)
4. E. Garcia-Berro, J. Isern, Y.A. Kubyshin, Astronomical measurements and constraints on the variability of fundamental constants. Astron. Astrophys. Rev. **14**, 113 (2007). https://doi.org/10.1007/s00159-006-0004-8
5. P.J. Mohr, B.N. Taylor, D.B. Newell, Codata recommended values of the fundamental physical constants: 2006. Rev. Mod. Phys. **80**, 633–730 (2008). https://doi.org/10.1103/RevModPhys.80.633
6. T.D. Le, Probing proton-to-electron mass ratio variability with QSO 0347-383 spectra. J. High Energy Astrophys. **44**, 74–78 (2024). https://doi.org/10.1016/j.jheap.2024.08.005
7. E. Garcia-Berro, Y. Kubyshin, P. Loren-Aguilar, J. Isern, The variation of the gravitational constant inferred from the Hubble diagram of type Ia supernovae. Int. J. Mod. Phys. D **15**(08), 1163–1174 (2006). https://doi.org/10.1142/S0218271806008772
8. T.D. Le, Cosmological variation of the proton-to-electron mass ratio constrained by strong gravitational fields. Int. J. Mod. Phys. D 0(0), 2450013. https://doi.org/10.1142/S0218271824500135
9. J. Muller, L. Biskupek, Variations of the gravitational constant from lunar laser ranging data. Class. Quantum Gravity **24**, 4533–4538 (2007). https://doi.org/10.1088/0264-9381/24/17/017
10. E. Gaztanaga, E. Garcia-Berro, J. Isern, E. Bravo, I. Dominguez, Bounds on the possible evolution of the gravitational constant from cosmological type Ia supernovae. Phys. Rev. D **65**, 023506 (2002). https://doi.org/10.1103/PhysRevD.65.023506. arXiv:astro-ph/0109299
11. C.J. Copi, A.N. Davis, L.M. Krauss, New nucleosynthesis constraint on the variation of g. Phys. Rev. Lett. **92**, 171301 (2004). https://doi.org/10.1103/PhysRevLett.92.171301
12. M. Biesiada, B. Malec, A new white dwarf constraint on the rate of change of the gravitational constant. Mon. Not. Roy. Astron. Soc. **350**, 644 (2004). https://doi.org/10.1111/j.1365-2966.2004.07677.x. arXiv:astro-ph/0303489
13. O.G. Benvenuto, E. Garcia-Berro, J. Isern, Asteroseismological bound on G/G from pulsating white dwarfs. Phys. Rev. D **69**, 082002 (2004). https://doi.org/10.1103/PhysRevD.69.082002
14. S. Xu, M. Jura, D. Koester, B. Klein, B. Zuckerman, Elemental compositions of two extrasolar rocky planetesimals*. Astrophys. J. **783**(2), 79 (2014). https://doi.org/10.1088/0004-637X/783/2/79
15. S. Xu, M. Jura, D. Koester, B. Klein, B. Zuckerman, Discovery of molecular hydrogen in white dwarf atmospheres. Astrophys. J. Lett. **766**(2), 18 (2013). https://doi.org/10.1088/2041-8205/766/2/L18
16. E.J. Salumbides, M.L. Niu, J. Bagdonaite, N. Oliveira, D. Joyeux, L. Nahon, W. Ubachs, CO A–X system for constraining cosmological drift of the proton-electron mass ratio. Phys. Rev. A **86**, 022510 (2012). https://doi.org/10.1103/PhysRevA.86.022510
17. J. Bagdonaite, W. Ubachs, M.T. Murphy, J.B. Whitmore, Analysis of molecular hydrogen absorption toward QSO b06425038 for a varying proton-to-electron mass ratio*. Astrophys. J. **782**(1), 10 (2014). https://doi.org/10.1088/0004-637X/782/1/10
18. E.J. Salumbides, J. Bagdonaite, H. Abgrall, E. Roueff, W. Ubachs, H_2 Lyman and Werner band lines and their sensitivity for a variation of the proton-electron mass ratio in the gravitational potential of white dwarfs. **450**(2), 1237–1245 (2015). https://doi.org/10.1093/mnras/stv656. arXiv:1412.6920 [physics.atom-ph]
19. T.D. Le, New limit on space-time variation of the proton-to-electron mass ratio using high-resolution spectra of white dwarf stars. J. High Energy Astrophys. **29**, 43–46 (2021). https://doi.org/10.1016/j.jheap.2021.01.001
20. T.D. Le, Wavelengths of [Fe II] from quasar j110325–264515 for a study of space-time variations in the fine-structure constant. Results Phys. **12**, 1035–1037 (2019). https://doi.org/10.1016/j.rinp.2018.12.086
21. T.D. Le, A search for the space-time variations in the proton-to-electron mass ratio using the [Fe II] transitions. Chin. J. Phys. **62**, 252–257 (2019). https://doi.org/10.1016/j.cjph.2019.10.007
22. T. Le, A study of space-time variation of the gravitational constant using high-resolution quasar spectra. Gen. Relativ. Gravit. **53**, 1–8 (2021)
23. E. Garcia-Berro, Y. Kubyshin, P. Loren-Aguilar, J. Isern, The variation of the gravitational constant inferred from the Hubble diagram of type Ia supernovae. Int. J. Mod. Phys. D **15**(08), 1163–1174 (2006). https://doi.org/10.1142/s0218271806008772
24. P. Lorn-Aguilar, E. Garca-Berro, J. Isern, Y.A. Kubyshin, Time variation of g and Â within models with extra dimensions. Class. Quantum Gravity **20**(18), 3885–3896 (2003). https://doi.org/10.1088/0264-9381/20/18/302
25. J.-P. Uzan, The fundamental constants and their variation: observational and theoretical status. Rev. Mod. Phys. **75**(2), 403–455 (2003). https://doi.org/10.1103/revmodphys.75.403
26. J.D. Barrow, A.A.H. Graham, General dynamics of varying-alpha universes. Phys. Rev. D (2013). https://doi.org/10.1103/physrevd.88.103513
27. J. Hu, Measuring the fine-structure constant on a white dwarf surface; a detailed analysis of Fe V absorption in G191–B2B. Mon. Not. Roy. Astron. Soc. **500**(1), 1466–1475 (2020). https://doi.org/10.1093/mnras/staa3066. arXiv:2007.10905 [astro-ph.SR]
28. E. García-Berro, S. Torres, L.G. Althaus, A.H. Córsico, P. Lorén-Aguilar, A.D. Romero, J. Isern, White dwarf constraints on a varying G. Mem. Soc. Astron. It. **85**(1), 118–123 (2014). arXiv:1308.5414 [astro-ph.SR]
29. M.T. Clara, C.J.A.P. Martins, Primordial nucleosynthesis with varying fundamental constants. Improved constraints and a possible solution to the lithium problem. **633**, 11 (2020). https://doi.org/10.1051/0004-6361/201937211. arXiv:2001.01787 [astro-ph.CO]
30. C.J.A.P. Martins, M. Vila Miñana, Consistency of local and astrophysical tests of the stability of fundamental constants. Phys. Dark Univ. **25**, 100301 (2019). https://doi.org/10.1016/j.dark.2019.100301
31. J. Bagdonaite, M. Daprà, P. Jansen, H.L. Bethlem, W. Ubachs, S. Muller, C. Henkel, K.M. Menten, Robust constraint on a drifting proton-to-electron mass ratio at $z = 0.89$ from methanol observation at three radio telescopes. Phys. Rev. Lett. **111**, 231101 (2013). https://doi.org/10.1103/PhysRevLett.111.231101
32. M.T. Clara, C.J.A.P. Martins, Primordial nucleosynthesis with varying fundamental constants: Improved constraints and a pos-

sible solution to the lithium problem. Astron. Astrophys. **633**, 11 (2020). https://doi.org/10.1051/0004-6361/201937211
33. A. Hees, T. Do, B. Roberts, A. Ghez, S. Nishiyama, R. Bentley, A. Gautam, S. Jia, T. Kara, J. Lu, H. Saida, S. Sakai, M. Takahashi, Y. Takamori, Search for a variation of the fine structure constant around the supermassive black hole in our galactic center. Phys. Rev. Lett. (2020). https://doi.org/10.1103/physrevlett.124.081101
34. S. Seager, G. Mallén-Ornelas, A unique solution of planet and star parameters from an extrasolar planet transit light curve. **585**(2), 1038–1055 (2003). https://doi.org/10.1086/346105. arXiv:astro-ph/0206228 [astro-ph]
35. R.P. van der Marel, M. Franx, A new method for the identification of non-Gaussian line profiles in elliptical galaxies. **407**, 525 (1993). https://doi.org/10.1086/172534
36. T. Le, White dwarf spectra for studies of time variation of the fine structure constant. Braz. J. Phys. **49**(2), 256–261 (2019)
37. T.D. Le, Updated constraints on the variations of the fine-structure constant from an analysis of white-dwarf spectra. Symmetry (2019). https://doi.org/10.3390/sym11070936
38. J. Bagdonaite, W. Ubachs, M.T. Murphy, J.B. Whitmore, Constraint on a varying proton-electron mass ratio 1.5 billion years after the big bang. Phys. Rev. Lett. **114**, 071301 (2015). https://doi.org/10.1103/PhysRevLett.114.071301
39. J. Magueijo, J.D. Barrow, H.B. Sandvik, Is it e or is it c? Experimental tests of varying alpha. Phys. Lett. B **549**(3), 284–289 (2002). https://doi.org/10.1016/S0370-2693(02)02928-3
40. M. Jamil, E.N. Saridakis, M.R. Setare, Holographic dark energy with varying gravitational constant. Phys. Lett. B **679**(3), 172–176 (2009). https://doi.org/10.1016/j.physletb.2009.07.048
41. C.M. Will, The confrontation between general relativity and experiment. Living Rev. Relativ. **17**, 4 (2014). https://doi.org/10.12942/lrr-2014-4. arXiv:1403.7377 [gr-qc]
42. N. Yunes, F. Pretorius, D. Spergel, Constraining the evolutionary history of newton's constant with gravitational wave observations. Phys. Rev. D **81**, 064018 (2010). https://doi.org/10.1103/PhysRevD.81.064018
43. T. Damour, G.W. Gibbons, J.H. Taylor, Limits on the variability of *g* using binary-pulsar data. Phys. Rev. Lett. **61**, 1151–1154 (1988). https://doi.org/10.1103/PhysRevLett.61.1151
44. T. Damour, J.H. Taylor, On the orbital period change of the binary pulsar PSR 1913+16. **366**, 501 (1991). https://doi.org/10.1086/169585
45. I.L. Shapiro, J. Sola, On the possible running of the cosmological 'constant'. Phys. Lett. B **682**, 105–113 (2009). https://doi.org/10.1016/j.physletb.2009.10.073. arXiv:0910.4925 [hep-th]
46. V.M. Kaspi, J.H. Taylor, M.F. Ryba, High-precision timing of millisecond pulsars. III. Long-term monitoring of PSRs B1855+09 and B1937+21. **428**, 713 (1994). https://doi.org/10.1086/174280
47. S.E. Thorsett, The gravitational constant, the Chandrasekhar limit, and neutron star masses. Phys. Rev. Lett. **77**, 1432–1435 (1996). https://doi.org/10.1103/PhysRevLett.77.1432
48. D.B. Guenther, L.M. Krauss, P. Demarque, Testing the constancy of the gravitational constant using helioseismology. **498**(2), 871–876 (1998). https://doi.org/10.1086/305567
49. J.P.W. Verbiest, M. Bailes, W. Straten, G.B. Hobbs, R.T. Edwards, R.N. Manchester, N.D.R. Bhat, J.M. Sarkissian, B.A. Jacoby, S.R. Kulkarni, Precision timing of PSR J0437-4715: an accurate pulsar distance, a high pulsar mass and a limit on the variation of Newton's gravitational constant. Astrophys. J. **679**, 675–680 (2008). https://doi.org/10.1086/529576. arXiv:0801.2589 [astro-ph]
50. S.A. Levshakov, M. Centurión, P. Molaro, S. d'Odorico, D. Reimers, R. Quast, M. Pollmann, Most precise single redshift bound to. Astron. Astrophys. **449**(3), 879–889 (2006)
51. S.A. Levshakov, M. Dessauges-Zavadsky, S. D'Odorico, P. Molaro, A new constraint on cosmological variability of the proton-to-electron mass ratio. Mon. Not. Roy. Astron. Soc. **333**(2), 373–377 (2002). https://doi.org/10.1046/j.1365-8711.2002.05408.x https://arxiv.org/abs/academic.oup.com/mnras/article-pdf/333/2/373/18413228/333-2-373.pdf
52. S.A. Levshakov, P. Molaro, S. Lopez, S. D'Odorico, M. Centurión, P. Bonifacio, I.I. Agafonova, D. Reimers, A new measure of $\Delta\alpha/\alpha$ at redshift z = 1.84 from very high resolution spectra of q 1101–264*. AA **466**(3), 1077–1082 (2007). https://doi.org/10.1051/0004-6361:20066064
53. S.A. Levshakov, D. Reimers, M.G. Kozlov, S.G. Porsev, P. Molaro, A new approach for testing variations of fundamental constants over cosmic epochs using fir fine-structure lines. AA **479**(3), 719–723 (2008). https://doi.org/10.1051/0004-6361:20079116
54. S.A. Levshakov, A.V. Lapinov, C. Henkel, P. Molaro, D. Reimers, M.G. Kozlov, I.I. Agafonova, Searching for chameleon-like scalar fields with the ammonia method – ii. Mapping of cold molecular cores in NH3 and HC3N lines. AA **524**, 32 (2010). https://doi.org/10.1051/0004-6361/201015332
55. S.A. Levshakov, P. Molaro, A.V. Lapinov, D. Reimers, C. Henkel, T. Sakai, Searching for chameleon-like scalar fields with the ammonia method*. AA **512**, 44 (2010). https://doi.org/10.1051/0004-6361/200913007
56. S.A. Levshakov, M.G. Kozlov, D. Reimers, Methanol as a tracer of fundamental constants. Astrophys. J. **738**(1), 26 (2011). https://doi.org/10.1088/0004-637X/738/1/26
57. S.A. Levshakov, M.G. Kozlov, I.I. Agafonova, Constraints on the electron-to-proton mass ratio variation at the epoch of reionization. Mon. Not. Roy. Astron. Soc. **498**(3), 3624–3632 (2020). https://doi.org/10.1093/mnras/staa2635. arXiv:2008.11143 [astro-ph.CO]
58. S. Truppe, R.J. Hendricks, S.K. Tokunaga, H.J. Lewandowski, M.G. Kozlov, C. Henkel, E.A. Hinds, M.R. Tarbutt, A search for varying fundamental constants using hertz-level frequency measurements of cold CH molecules. Nat. Commun. **4**, 2600 (2013). https://doi.org/10.1038/ncomms3600. arXiv:1308.1496 [physics.atom-ph]
59. J.D. Anderson, G. Schubert, V. Trimble, M.R. Feldman, Measurements of newton's gravitational constant and the length of day. Europhys. Lett. **110**(1), 10002 (2015). https://doi.org/10.1209/0295-5075/110/10002
60. E.P. Bellinger, J. Christensen-Dalsgaard, Asteroseismic constraints on the cosmic-time variation of the gravitational constant from an ancient main-sequence star. Astrophys. J. Lett. **887**(1), 1 (2019). https://doi.org/10.3847/2041-8213/ab43e7. arXiv:1909.06378 [astro-ph.SR]
61. J. Lu, E.N. Saridakis, M.R. Setare, L. Xu, Observational constraints on holographic dark energy with varying gravitational constant. JCAP **03**, 031 (2010). https://doi.org/10.1088/1475-7516/2010/03/031. arXiv:0912.0923 [astro-ph.CO]
62. C.J.A.P. Martins, A.M.M. Pinho, Stability of fundamental couplings: a global analysis. Phys. Rev. D **95**, 023008 (2017). https://doi.org/10.1103/PhysRevD.95.023008
63. T. Le, Searching for a secular variation of the gravitational constant using strong gravitational fields. Gen. Relativ. Gravit. **55**(11), 124 (2023)
64. M.C. Ferreira, O. Frigola, C.J.A.P. Martins, A.M.R.V.L. Monteiro, J. Solà, Consistency tests of the stability of fundamental couplings and unification scenarios. Phys. Rev. D **89**, 083011 (2014). https://doi.org/10.1103/PhysRevD.89.083011
65. A. Coc, N.J. Nunes, K.A. Olive, J.-P. Uzan, E. Vangioni, Coupled variations of fundamental couplings and primordial nucleosynthesis. Phys. Rev. D **76**, 023511 (2007). https://doi.org/10.1103/PhysRevD.76.023511
66. J.A. King, M.T. Murphy, W. Ubachs, J.K. Webb, New constraint on cosmological variation of the proton-to-electron mass ratio from Q0528250. Mon. Not. Roy. Astron. Soc. **417**(4), 3010–3024 (2011). https://doi.org/10.1111/j.1365-2966.2011.19460.

x https://arxiv.org/abs/academic.oup.com/mnras/article-pdf/417/4/3010/17329919/mnras0417-3010.pdf
67. E. Garcia-Berro, P. Loren-Aguilar, S. Torres, L.G. Althaus, J. Isern, An upper limit to the secular variation of the gravitational constant from white dwarf stars. JCAP **05**, 021 (2011). https://doi.org/10.1088/1475-7516/2011/05/021. arXiv:1105.1992 [gr-qc]
68. H. Fritzsch, The fundamental constants in physics and their time dependence. Prog. Part. Nucl. Phys. **61**, 329–342 (2008). https://doi.org/10.1016/j.ppnp.2008.03.001. arXiv:0802.0099 [hep-ph]
69. T.D. Le, Exploring secular variation of the gravitational constant from high-resolution quasar spectra. Sci. Rep. **14**(1), 15610 (2024). https://doi.org/10.1038/s41598-024-65484-5
70. T.D. Le, Probing secular changes in the gravitational constant with white dwarf spectra. Eur. Phys. J. C **84**(7), 698 (2024). https://doi.org/10.1140/epjc/s10052-024-13025-9